Effects of fullerene addition on the thermo-optical properties of smectic liquid crystals at the vicinity of the nematic–smectic-*A* phase transition

Lidiane Omena, Pedro B. de Melo, Maria S. S. Pereira, and Italo N. de Oliveira

Instituto de Física, Universidade Federal de Alagoas 57072-970 Maceió-AL, Brazil

The present work is devoted to the study of the thermo-optical properties of liquid crystals doped with traces of fullerene C_{60} at the vicinity of the nematic–smectic-*A* phase transition. By using the time-resolved *Z*-scan technique, we measure the temperature dependence of the thermo-optical coefficient and the thermal diffusivity. Our results reveal that the critical behavior of the thermal diffusivity is strongly affected by the fullerene addition. We provide a detailed discussion under the light of the distinct mechanisms behind the thermal transport in liquid-crystal samples.

I. INTRODUCTION

The characterization of phase transitions and critical phenomena involving liquid crystals constitutes a challenging topic in soft-matter physics, being a subject of theoretical and experimental investigations for several decades [1–5]. Indeed, liquid-crystalline systems exhibit a large variety of unusual phase sequences which are strongly affected by external fields [6,7], surface anchoring [8], confinement [9], and finite-size effects [10]. In this context, the smectic-*A* (Sm*A*) to nematic (*N*) phase transition plays an important role due to the rich phenomenology associated with the continuous or discontinuous nature of such transition, which is determined by the nematic range of the investigated compound [11–13]. In particular, the nematic range of smectogenic compounds reflects the coupling strength between the nematic and smectic order parameters that delimits the crossover from continuous to discontinuous transition via a Gaussian tricritical point [11]. As a consequence, the equilibrium and dynamical thermal parameters may exhibit an isotropic or a weakly anisotropic critical behavior at the *N*-Sm*A* transition [11,14]. In fact, the study of the effective critical behavior of thermal parameters of liquid crystals has attracted a renewed interest due to their major relevance for electro-optical devices based on electronic and optical properties of liquid-crystal samples [15].

It is well known that the introduction of guest particles may induce dramatical changes in the phase transitions of liquid-crystal hosts [16–20]. A prominent example is the pronounced shift in nematic-isotropic and smectic-nematic transition temperatures due to the addition of ferroelectric nanoparticles [16,17,20]. In particular, it was observed that the local electric field of guest particles reinforces the nematic order parameter, resulting in the enhancement of nematic-isotropic transition temperature [16,21]. However, it was demonstrated that this effect only persists at small concentrations of ferroelectric nanoparticles; otherwise, the particles-induced inhomogeneity becomes predominant and the transition temperatures tend to decrease as a typical quenched disorder phenomenon [17,20]. The reduction of nematic–smectic-*A* transition temperature has also been reported for liquid-crystal samples doped with azo-dyes [19] or containing nonmesogenic impurities [22,23]. Concerning the critical behavior at the nematic–smectic-*A* phase transition, high-resolution calorimetric studies revealed that the critical exponent of specific heat is sensitive to the concentration and coating of guest magnetic particles [18]. Similar results were obtained for critical exponents of the elastic constant and rotational viscosity by using dynamic light scattering in a liquid-crystalline system containing ferroelectric nanoparticles at the vicinity of the nematic–smectic-*A* phase transition [17].

Recently, special attention has been devoted to the control and amplification of the electronic and optical properties of liquid crystals due to their potential application in optical devices [24–26]. Among the great variety of methods used to modify the properties of liquid-crystal matrices, the addition of electron donor-acceptor molecules has been demonstrated as an excellent alternative for electro-optical purposes, such as data storage and coherent image amplification [25–28]. In particular, it has been reported that the insertion of fullerene C_{60} in nematic liquid crystals leads to a dramatic improvement of the photorefractive response of the samples, being characterized by a large enhancement in the diffraction efficiency of writing beams [29–32]. Indeed, fullerene C_{60} enhances the photocharge generation in nematic samples due to the formation of charge-transfer complexes upon photoexcitation, contributing to the formation of a space-charged field that is responsible for the spatial modulation of the refractive index [26,28]. Further, the introduction of fullerene has also been used to modify the structural organization of cholesteric samples from the formation of twist-bond defects upon low-intensity illumination [33]. Concerning the thermal properties, polarizing optical microscopy and differential scanning calorimetry investigations have not identified any significant contribution associated with the fullerene addition at the nematic-isotropic phase transition [34]. Although the effects associated with the addition of fullerene on the optical properties of nematic liquid crystals have been widely explored, thermal parameters of smectic liquid crystals doped with fullerene have not been investigated so far.

In the present work, we study the thermo-optical properties of liquid crystals doped with traces of fullerene C_{60} at the vicinity of the nematic–smectic-*A* phase transition. By using the time-resolved *Z*-scan technique, we measure the temperature dependence of the thermo-optical coefficient and the thermal diffusivity of pure and fullerene-doped 8CB samples. Our results show that the introduction of fullerene affects the Sm*A*-*N* transition temperature, as well as the heat diffusion of liquid-crystal hosts, especially at the smectic

phase. Further, we analyze the effects of fullerene addition in the critical behavior of thermal diffusivity under light of the mechanisms behind the heat transport in smectic samples.

II. MATERIAL AND METHODS

We chose the compound 4-octyl-4′-cyanobiphenyl (8CB) as our liquid-crystal sample. It presents an isotropic-nematic phase transition at $T_{NI} = 313.5$ K and a nematic–smectic-A transition at $T_{AN} = 306.5$ K. This compound exhibits a good chemical stability upon laser exposure and it was purchased from Sigma-Aldrich, being used without further purification. The fullerene C_{60} was also purchased from Sigma-Aldrich and its concentration in the liquid-crystal samples was varied in the range of 0–0.4 wt. %. No phase separation was observed at these concentrations. Homeotropic samples were prepared by treating cleaned glass surfaces with surfactant. Spacers were used to maintain the cell thickness at $\ell_0 = 100$ μm. The cells were filled by capillarity action in the isotropic phase of 8CB ($T \approx 323$ K) and slowly cooled down to room temperature. Samples were observed under a crossed-polarized microscope to ensure alignment and uniformity. Samples were placed in a temperature-controlled oven within the accuracy of 0.1 K, with the sample temperature being varied in steps of $\Delta T = 0.2$ K, in a rate of 0.1 K/min. After reaching the target temperature, the measurement was performed after a waiting time of 20 min in order to certify that the system has reached the equilibrium configuration.

The time-resolved Z-scan technique was implemented using a linear polarized cw diode-pumped solid-state (DPSS) laser at $\lambda = 532$ nm as the light source. The laser beam presented a Gaussian profile with a well-defined vertical polarization and the laser power used to excite the sample was $P = 0.8$–1.7 mW. The laser beam was focused by a lens with a focal length of 15 cm, which provided a minimum waist of $w_0 = 40$ μm, resulting in a confocal distance $z_c = 9.45$ mm. A mechanical chopper was used to modulate the laser beam, producing square-wave pulses with a duration of 70 ms. The sample was excited at normal incidence in order to avoid reorientation of the orientational order. The sample was moved back and forth along the z axis around the beam waist of the laser during the measurement, with a single displacement step of 5 mm.

III. THERMAL LENS BACKGROUND

The time-resolved Z-scan technique is an efficient method to investigate the thermal properties in low absorbing liquid-crystal samples from the emergence of the thermal lens effect [35,36]. In particular, the thermal lens effect consists in the conversion of the absorbed energy into heat when a Gaussian laser beam passes through the sample, which behaves itself as a lenslike optical element due to the temperature-induced change in the optical path. More specifically, the local heating of the liquid-crystal sample modifies its birefringence, resulting in a self-focusing or defocusing of the beam center. Further, the formation time of the thermal lens can be used to determine the thermal diffusivity of the sample [35]. By considering the aberration model to describe the optical path

change in the thermal lens effect, the transient transmittance in the far field can be expressed as [37]

$$I(\tau) = I(0) \left\{ 1 - \frac{\theta}{2} \tan^{-1} \left[\frac{2\gamma}{(3 + \gamma^2) + (9 + \gamma^2)\left(\frac{\tau_c}{2\tau}\right)} \right] \right\}^2,$$
(1)

with $\gamma = z/z_c$, where z is the sample position in relation to the position of minimum beam waist ($z = 0$) and z_c is the confocal parameter. θ is the thermal-induced phase shift of the beam wave front after it passage through the sample. τ is the exposure time of the sample during each square pulse, while τ_c is the characteristic time for the formation of the thermal lens. The parameters τ_c and θ can be directly obtained from the fitting of the experimental data for the transient transmittance by using Eq. (1). θ and τ_c are free parameters which can be associated with the sample and experimental setup parameters as follows:

$$\theta = -\left[\frac{P_i A \ell_0}{\kappa \lambda} \right] \frac{dn_o}{dT}$$
(2)

and

$$\tau_c = \frac{w^2}{4D}.$$
(3)

Here, w is the beam radius at the sample, defined as $w = w_0\sqrt{1 + \gamma^2}$, and D is the thermal diffusivity. P_i is the incident laser power, A is the absorption coefficient at the excitation wavelength, and κ is the thermal conductivity. n_o is the ordinary refractive index of the liquid-crystal samples, which can be defined as [38]

$$n_o = \bar{n} - \tfrac{1}{3}\Delta n(T),$$
(4)

where $\bar{n}$ is the average refractive index and $\Delta n(T)$ is the liquid-crystal birefringence, which exhibits a strong dependence on the sample temperature T, due to its relation with the orientational order parameter [38]. Previous works have reported that the average refractive index exhibits a linear decrease as the temperature is enhanced, with $d\bar{n}/dT \approx -10^{-4}$K^{-1} [38]. Once such a contribution is around two orders of magnitude lower than the variation rate of the liquid-crystal birefringence with temperature $[d\Delta n(T)/dT]$, the thermal variations in the optical path are mainly associated with the variation in the birefringence of liquid-crystal samples. As a consequence, the temperature effects on the beam phase shift θ can be directly attributed to the birefringent thermo-optical coefficient. In what follows, we will use the above description to analyze the effects of the fullerene addition on the thermo-optical properties of liquid crystals close to the nematic–smectic-A phase transition.

IV. RESULTS

In Fig. 1 we show the time evolution of the far-field transmittance for pure 8CB samples and 8CB liquid crystals doped with fullerene at a concentration of 0.1 wt. %. The transient transmittances were recorded for distinct temperatures of samples placed at the position $z = \sqrt{3}z_c$. For the undoped sample, one can observe that a self-focusing behavior ($d\Delta n/dT < 0$) takes place at the nematic and smectic phases
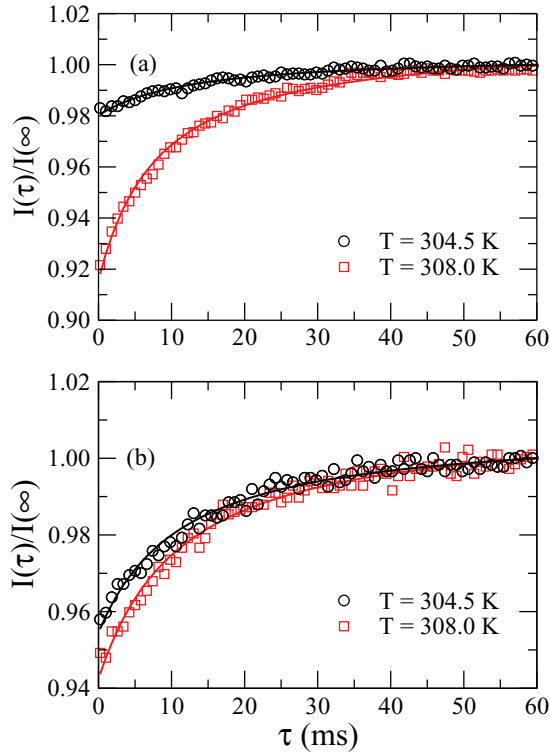
FIG. 1. (Color online) Transient intensities of time-resolved Z-scan measurements in (a) pure 8CB and (b) fullerene-doped 8CB samples at distinct temperatures: $T = 308$ K (red squares) and $T = 304.5$ K (black circles), corresponding to nematic and smectic phases, respectively. The concentration of fullerene in the doped sample was $c = 0.1$ wt. %. Solid lines represent the fitting curves using Eq. (1). In both cases, we observe that the phase shift is less pronounced in the smectic phase.
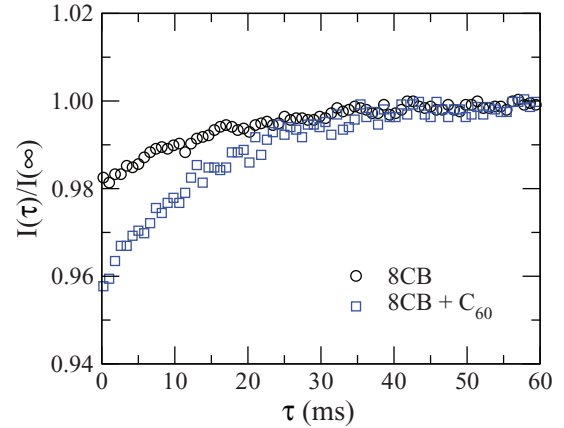

FIG. 2. (Color online) Transient intensities of pure (black circles) and fullerene-doped (blue squares) 8CB samples at the smectic phase, with $T = 304.5$ K. The concentration of fullerene in the doped sample was $c = 0.1$ wt. %. Although the phase shift is higher in the doped sample, one can notice that the steady-state regime is reached faster in such a system, indicating that the addition of fullerene reduces the characteristic time for the formation of the thermal lens.

that is characterized by the increase of the far-field transmittance with the exposure time ($\theta < 0$), as shown in Fig. 1(a). We notice that the phase shift is smaller in the smectic phase, with a slow relaxation to the steady-state regime in both phases. Indeed, the temperature-induced changes in the liquid-crystal birefringence are more pronounced in the nematic phase. This feature is due to the fact that the smectic phase exhibits an additional quasi-long-range translational order. Although the smectic layers impose restrictions to the molecular motion through them, it has been demonstrated that the thermal conductivity is slightly affected by the emergence of the layered structure [39,40], which exhibits a small discontinuity due to the coupling between smectic and nematic order parameters [40,41]. A similar behavior is observed in the fullerene-doped 8CB sample, with the self-focusing of the laser beam ($\theta < 0$) and a smaller phase shift in the smectic phase when compared with the nematic one, as exhibited in Fig. 1(b). However, the evolution to the steady-state regime in the smectic phase seems to be affected by the fullerene addition, with a reduction of the characteristic time for the formation of the thermal lens and the heat diffusion occurring in a more efficient way.

Let us now characterize the effects of the fullerene addition on the thermal properties of smectic phase. In Fig. 2, we present a comparison between the transient intensities of pure

and fullerene-doped 8CB sample at $T = 304.5$ K, well below the SmA-N transition temperature. Here, one can clearly note that the steady-state regime is reached faster in the doped sample, indicating that the fullerene guest increases the heat diffusion in the smectic phase. In fact, the addition of fullerene enhances the mean free path of hydrodynamic modes responsible for the heat conduction in the liquid-crystal samples, once the mean diameter of the fullerene balls ($d_f \approx 7$ Å) is almost five times smaller than the smectic layer thickness ($d_s \approx 32$ Å). It is important to stress that the transient in the far-field transmittance at normal incidence is associated with the thermal diffusion, because the optical torque responsible for the director reorientation is null at this excitation geometry [42].

Using Eq. (1), one can obtain the phase shift and the thermal diffusivity of pure and fullerene-doped 8CB samples by fitting the time evolution of the far-field transmittance. In Fig. 3, we exhibit the temperature dependence of the phase shift θ at the vicinity of the nematic–smectic-A phase transition. Again, we consider pure and fullerene-doped 8CB samples. The phase shifts were rescaled by the power of the incident laser beam in order to allow a better analysis of the photothermal process. In the pure 8CB sample, one can note that the absolute value of the phase shift decreases as the temperature is reduced, but a small discontinuity is observed at the nematic–smectic-A transition temperature, as shown in Fig. 3(a). Such a behavior is associated with the strong coupling between the thermal fluctuations of the optical axis and the smectic order parameter, once the phase shift reflects the rate of variation of the sample birefringence with temperature, as defined in Eq. (2). In fact, the nematic–smectic-A phase transition presents a crossover from continuous to tricritical behavior in compounds exhibiting a small nematic range, which is characterized by a McMillan ratio $0.93 < T_{AN}/T_{NI} < 1$ [11,14,40]. Indeed, the McMillan ratio for 8CB is $T_{AN}/T_{NI} = 0.977$, and a small discontinuity in nematic order parameter may take
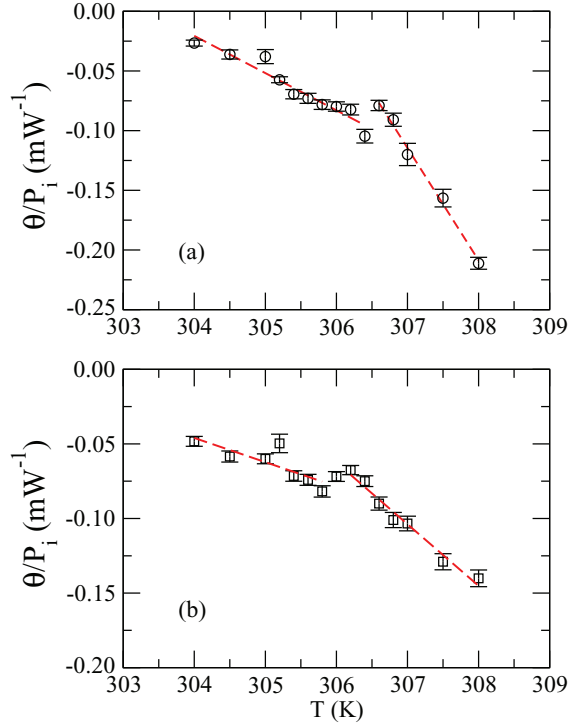
FIG. 3. (Color online) Beam phase shift in units of the incident laser power as a function of the temperature, for (a) pure 8CB sample and (b) 8CB containing fullerene at a concentration of 0.1 wt. %. Red dashed lines are just to guide the eyes. Notice that the insertion of fullerene reduces the discontinuity associated with the nematic–smectic-A phase transition.

place at the transition, due to the coupling between smectic order parameter and the thermal fluctuations in the nematic order [43]. As a consequence, an abrupt change in the slope $d\Delta n/dT$ is observed at the transition temperature, resulting in a discontinuous variation of the thermo-optical coefficient. For the 8CB sample doped with fullerene ($c = 0.1$ wt. %), we observe that the discontinuity at the phase transition is reduced, which takes place at a temperature slightly lower than the transition temperature T_{AN} of the pure 8CB sample. Further, we notice that the addition of fullerene at this concentration induces a small enhancement in the absolute value of beam phase shift in the smectic phase.

In order to determine the effects of fullerene addition in the SmA-N phase transition, we exhibit in Fig. 4 the transition temperature, $T_{AN}(c)$, as a function of the fullerene concentration. The transition temperatures were estimated from the polarized optical microscopy of the samples. As one can notice, the SmA-N transition temperature presents a linear decrease as the concentration of fullerene is enhanced, indicating that the introduction of such a nonmesogenic compound modifies the effective interaction that gives rise to the smectic phase. Indeed, previous works have reported that the addition of nonmesogenic materials in the liquid-crystal sample tends to reduce the SmA-N transition temperature [22], due to the emergence of an additional term in the free energy associated with the coupling between the smectic order parameter and the solute concentration. More specifically, it was shown that $T_{AN}(c) = T_{AN}(0) - \Gamma c$, where $T_{AN}(0)$
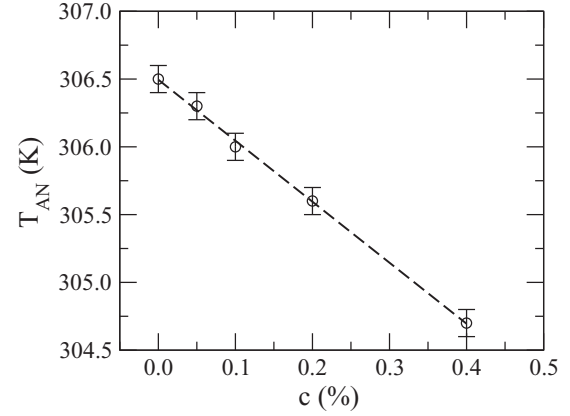

FIG. 4. Smectic-nematic transition temperature as a function of the fullerene weight concentration. The dashed line is the linear regression using the expression $T_{AN}(c) = T_{AN}(0) - \Gamma c$.

is the transition temperature of the pure sample and Γ is a coefficient representing the coupling between smectic order parameter and the concentration of the nonmesogenic guest [22,23].

In Fig. 5, we present the effective thermal diffusivity as a function of the reduced temperature, $t = [T - T_{AN}(c)]/T_{AN}(c)$, for pure and fullerene-doped ($c = 0.1$ wt. %)
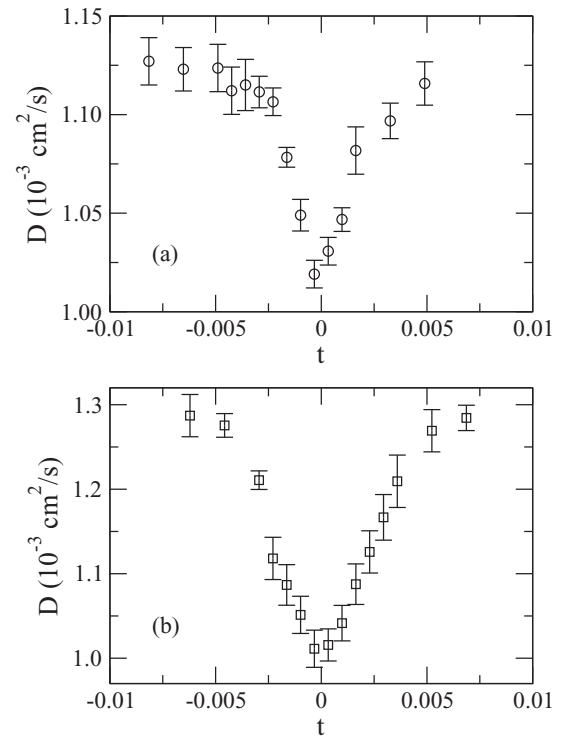

FIG. 5. Temperature dependence of the effective thermal diffusivity of (a) pure and (b) fullerene-doped 8CB samples at the vicinity of the nematic–smectic-A phase transition. The concentration of fullerene in the doped sample was $c = 0.1$ wt. %. Notice that the addition of fullerene does not modify the vanishing critical behavior of the thermal diffusivity at the SmA-N phase transition, indicating that heat diffusion is governed by short-range processes.

8CB samples. The thermal diffusivity was computed by using Eq. (3), from the estimation of the characteristic time for the formation of the thermal lens during the laser exposure. In a pure 8CB sample, it is observed that the effective thermal diffusivity exhibits a critical behavior at the nematic–smectic-*A* phase transition, vanishing at the transition temperature. Such behavior is similar to that reported by previous works using photopyroelectric and thermal wave techniques [14,15]. In particular, the vanishing critical behavior of the thermal diffusivity is usually associated with the divergence of the specific heat at the transition, while the thermal conductivity stays finite [14]. In fact, the divergence of the correlation length and the emergence of long-range correlations does not affect the thermal conductivity, which is governed by short-range processes [44]. A similar scenario is observed in Fig. 5(b), with the thermal diffusivity presenting a critical vanishing at the transition temperature of the doped sample. Although the fullerene inclusion is expected to suppress the critical divergence of the specific heat similar to that reported for 8CB containing small quartz spheres at very low concentrations [45], the vanishing critical behavior of the thermal diffusivity still holds. In this case, the addition of fullerene does not favor a nondissipative coupling between Goldstone modes whose relaxation rates go to zero as the correlation length diverges, which would give rise to a divergent critical behavior of the thermal conductivity at the nematic–smectic-*A* phase transition [46]. At temperatures where the smectic order is well established ($t < -0.005$), we can notice that the thermal diffusivity is higher in the fullerene-doped sample than in the pure one, indicating the enhancement in the heat diffusion due to the fullerene addition.

V. SUMMARY AND CONCLUSIONS

In summary, we have studied the effects of the addition of fullerene in the thermo-optical properties of 8CB liquid-crystal samples at the vicinity of the nematic–smectic-*A* phase transition. By using the time-resolved *Z*-scan technique, we characterized the formation of a thermal lens in pure and doped samples. Our results showed that the addition of fullerene induces a reduction in the nematic–smectic-*A* transition temperature, which may be attributed to the emergence of a coupling between the smectic order parameter and the concentration of guest particles. Similar results have been reported for 8CB samples containing distinct nonmesogenic impurities [22,23]. Further, we showed that the critical vanishing behavior of the thermal diffusivity still holds as the fullerene is added in liquid-crystal samples. Such a result indicates that the insertion of such guest particles does not favor a nondissipative coupling between long-lived Goldstone modes, with the heat diffusion being governed by short-range processes. The present results suggest that the insertion of fullerene may induce significant modifications in the thermo-optical properties of liquid-crystal samples, a feature that can be explored in future applications of such a guest-host system in electro-optical devices.

[1] P. G. de Gennes and J. Prost, *The Physics of Liquid Crystals* (Clarendon Press, Oxford, 1993).

[2] R. Pindak, W. O. Sprenger, D. J. Bishop, D. D. Osheroff, and J. W. Goodby, Phys. Rev. Lett. **48**, 173 (1982).

[3] T. Stoebe, P. Mach, and C. C. Huang, Phys. Rev. Lett. **73**, 1384 (1994).

[4] L. D. Pan, B. K. McCoy, S. Wang, W. Weissflog, and C. C. Huang, Phys. Rev. Lett. **105**, 117802 (2010).

[5] T. Ostapenko, D. B. Wiant, S. N. Sprunt, A. Jákli, and J. T. Gleeson, Phys. Rev. Lett. **101**, 247801 (2008).

[6] M. S. S. Pereira, M. L. Lyra, and I. N. de Oliveira, Phys. Rev. Lett. **103**, 177801 (2009).

[7] B. Wen and C. Rosenblatt, Phys. Rev. Lett. **89**, 195505 (2002).

[8] M. S. S. Pereira, I. N. de Oliveira, and M. L. Lyra, Phys. Rev. E **84**, 061706 (2011).

[9] Z. Kutnjak, S. Kralj, G. Lahajnar, and S. Zumer, Phys. Rev. E **68**, 021705 (2003).

[10] C. Bahr, Int. J. Mod. Phys. B **8**, 3051 (1994).

[11] C. W. Garland and G. Nounesis, Phys. Rev. E **49**, 2964 (1994).

[12] E. Anesta, G. S. Iannacchione, and C. W. Garland, Phys. Rev. E **70**, 041703 (2004).

[13] F. Beaubois, T. Claverie, J. P. Marcerou, J. C. Rouillon, H. T. Nguyen, C. W. Garland, and H. Haga, Phys. Rev. E **56**, 5566 (1997).

[14] M. Marinelli, F. Mercuri, S. Foglietta, U. Zammit, and F. Scudieri, Phys. Rev. E **54**, 1604 (1996).

[15] J. Morikawa, T. Hashimoto, A. Kishi, Y. Shinoda, K. Ema, and H. Takezoe, Phys. Rev. E **87**, 022501 (2013).

[16] F. Li, O. Buchnev, C. I. Cheon, A. Glushchenko, V. Reshetnyak, Y. Reznikov, T. J. Sluckin, and J. L. West, Phys. Rev. Lett **97**, 147801 (2006); **99**, 219901(E) (2007).

[17] A. Mertelj, L. Cmok, M. Copic, G. Cook, and D. R. Evans, Phys. Rev. E **85**, 021705 (2012).

[18] G. Cordoyiannis, L. K. Kurihara, L. J. Martinez-Miranda, C. Glorieux, and J. Thoen, Phys. Rev. E **79**, 011702 (2009).

[19] D. Bauman and H. Moryson, J. Mol. Struct. **404**, 113 (1997).

[20] A. Lorenz, N. Zimmermann, S. Kumar, D. R. Evans, G. Cook, M. F. Martínez, and H.-S. Kitzerow, J. Phys. Chem. B **117**, 937 (2013).

[21] L. M. Lopatina and J. V. Selinger, Phys. Rev. Lett. **102**, 197802 (2009).

[22] K. Denolf, B. Van Roie, C. Glorieux, and J. Thoen, Phys. Rev. Lett. **97**, 107801 (2006).

[23] K. Denolf, G. Cordoyiannis, C. Glorieux, and J. Thoen, Phys. Rev. E **76**, 051702 (2007).

[24] M. O'Neill and S. M. Kelly, Adv. Mater. **15**, 1135 (2003).

[25] F. Simoni and O. Francescangeli, J. Phys.: Condens. Matter **11**, R439 (1999).

[26] I. C. Khoo, Phys. Rep. **471**, 221 (2009).

[27] G. P. Wiederrecht, B. A. Yoon, and M. R. Wasielewski, Science **270**, 1794 (1995).

[28] O. Ostroverkhova and W. E. Moerner, Chem. Rev. **104**, 3267 (2004).

[29] I. C. Khoo, J. Ding, Y. Zhang, K. Chen, and A. Diaz, Appl. Phys. Lett. **82**, 3587 (2003).

[30] X. Sun, C. Ren, Y. Pei, and F. Yao, J. Phys. D **41**, 245105 (2008).

[31] X. Sun, Y. Pei, F. Yao, J. Zhang, and C. Hou, Appl. Phys. Lett. **90**, 201115 (2007).

[32] L. Song, W.-K. Lee, and X. Wang, Opt. Express **14**, 2197 (2006).

[33] O. Trushkevych, P. Ackerman, W. A. Crossland, and I. I. Smalyukh, Appl. Phys. Lett. **97**, 201906 (2010).

[34] H. Duran, B. Gazdecki, A. Yamashita, and T. Kyu, Liq. Cryst. **32**, 815 (2005).

[35] N. M. Kimura, A. de Campos, P. A. Santoro, M. Simes, S. L. Gómez, and A. J. Palangana, Phys. Lett. A **370**, 173 (2007).

[36] J. R. D. Pereira, A. M. Mansanares, A. J. Palangana, and M. L. Baesso, Phys. Rev. E **64**, 012701 (2001).

[37] C. A. Carter and J. M. Harris, Appl. Opt. **23**, 476 (1984).

[38] J. Li, S. Gauza, and S.-T. Wu, J. Appl. Phys. **96**, 19 (2004).

[39] F. Rondelez, W. Urbach, and H. Hervet, Phys. Rev. Lett. **41**, 1058 (1978).

[40] M. Marinelli, F. Mercuri, U. Zammit, and F. Scudieri, Phys. Rev. E **58**, 5860 (1998).

[41] U. Zammit, S. Paoloni, F. Mercuri, M. Marinelli, and F. Scudieri, AIP Adv. **2**, 012135 (2012).

[42] P. Oswald and P. Pieranski, *Nematic and Cholesteric Liquid Crystals* (CRC Press, Boca Raton, 2005).

[43] I. Lelidis, Phys. Rev. Lett. **86**, 1267 (2001).

[44] F. Mercuri, U. Zammit, and M. Marinelli, Phys. Rev. E **57**, 596 (1998).

[45] M. Marinelli, A. K. Ghosh, and F. Mercuri, Phys. Rev. E **63**, 061713 (2001).

[46] P. C. Hohenberg and B. I. Halperin, Rev. Mod. Phys. **49**, 435 (1977).